Flow sensing and energy harvesting characteristics of a wind-driven piezoelectric Pb(Zr0.52, Ti0.48)O₃ microcantilever

Huicong Liu[1,2], Songsong Zhang[2], Takeshi Kobayashi[3], Tao Chen[1], Chengkuo Lee[2]

[1]*Robotics and Microsystems Center and Collaborative Innovation Center of Suzhou Nano Science and Technology, Soochow University, Suzhou 215021, People's Republic of China*
[2]*Department of Electrical and Computer Engineering, National University of Singapore, 4 Engineering Drive 3, Singapore 117576, Singapore*
[3]*National Institute of Advanced Industrial Science and Technology (AIST), 1-2-1 Namiki, Tsukuba, Ibaraki 305-8564, Japan*
E-mail: elelc@nus.edu.sg

Wind flow regarded as a renewable energy source is present everywhere in indoor or open environments. A self-sustained flow-sensing microsystem is especially desirable in future applications of smart home, remote sensing and environmental monitoring. Piezoelectric thin films are commonly adopted in microenergy harvesters for converting the mechanical strain into an electrical charge based on the piezoelectric effect. It is also a promising candidate for flow sensors because of its passive nature, that is, the detectable output charge is a function of flow rate. The aim of this reported work has been to investigate the flow sensing and energy harvesting capabilities of a flexible piezoelectric Pb(Zr0.52, Ti0.48)O₃ (PZT) microcantilever under wind flow. A self-sustained flow-sensing microsystem is possible by integrating the arrays of PZT microcantilevers, which measure the flow rate of ambient wind by one microcantilever and scavenge wind-flow energy as a power source by the rest.

1. Introduction: There has been a growing demand for the deployment of autonomous flow-sensing microsystems in various applications such as smart home, remote area sensing and environmental monitoring [1–3]. A self-sustained flow-sensing microsystem requires a microflow sensor for sensing and monitoring, a control circuit for processing and communicating, as well as a self-sustained micropower source by scavenging energy from environment. Conventional microflow sensors require electrical power to measure thermal flux, mechanical strain, Coriolis force or capacitance with respect to flow velocity by operating thermal heaters, strain gauges, electromagnetic coils or capacitors [4–8]. Piezoelectric thin film is a promising candidate for flow sensing because of its passive nature for detecting output charge as a function of flow-induced deformation based on the piezoelectric effect. Hence, the flow-sensing capability of a piezoelectric Pb(Zr0.52, Ti0.48)O₃ (PZT) microcantilever is characterised in this Letter. Compared with conventional microflow sensors that have excitation and detection parts, the proposed piezoelectric-based one only has a detection part [9].

Harvesters from wind flow have been extensively developed because wind-flow energy is present everywhere in indoor and open environments. Besides the well-known approach of wind turbines [10–12], two types of vibration energy harvesters have been developed that rely on the drag force of the airflow [13–15] and the conversion of air motion to air steady oscillation [16–18], respectively. In both types of energy harvesters, piezoelectric thin film components are commonly adopted for converting kinetic energy into electricity.

The work reported in this Letter thus aimed to investigate the flow sensing and energy harvesting capabilities of a flexible piezoelectric PZT microcantilever from wind flow. The significance of this concept is that it does not exhibit the operation bandwidth issue of traditional vibration-based energy harvesters [19–21] and does not require an additional electrical energy for the excitation part as required in the traditional microflow sensors. Hence, by integrating the arrays of similar PZT microcantilevers, a self-sustained flow-sensing microsystem could be achieved in a way that one microcantilever measures the flow rate of ambient wind and the rest of the microcantilevers scavenge wind-flow energy as the power to sustain this microsystem.

2. Design and fabrication: Fig. 1 shows a schematic illustration of a piezoelectric PZT microcantilever immersed in a wind flow perpendicular to the cantilever surface. The PZT microcantilever consists of a Si beam (2 mm × 1.65 mm × 5 μm) coated with three PZT thin film components (denoted as 1, 2 and 3) and a Si proof mass (2 mm × 1.65 mm × 0.4 mm) connected at its free end. Each PZT thin film component has the same dimensions of 1.65 mm long and 0.6 mm wide. The outer frame of the PZT microcantilever is attached to a metal package base by a separating spacer. The top and bottom electrodes of each PZT
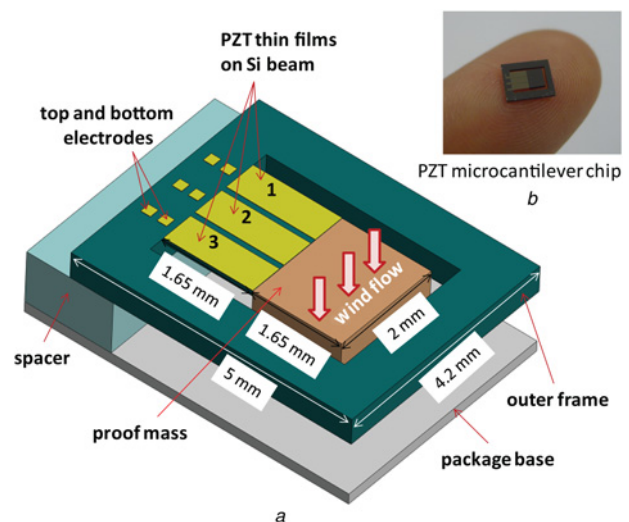

Figure 1 *Schematic illustration of a piezoelectric PZT microcantilever immersed in a wind flow*
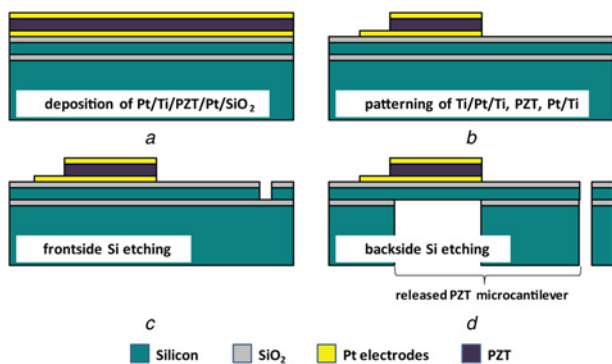
Figure 2 *Process flow of the PZT microcantilever*

Figure 4 *Schematic drawing of an air flow testing system*

thin film component are connected to their bonding pads of the metal package.

Fig. 2 shows the process flow. It starts from multilayer deposition of Pt/Ti/PZT/Pt/Ti/SiO$_2$ on a silicon-on-insulator (SOI) wafer with a 5 µm-thick structural Si layer, a 1 µm-thick buried oxide (BOX) layer and a 400 µm-thick handle Si layer. The SOI wafer is firstly oxidised at 1100°C to form a 1 µm-thick thermal oxide layer. After that, Pt (0.2 µm)/Ti (0.05 µm) thin films are deposited as the bottom electrode layer by DC magnetron sputtering. A 2.5 µm-thick PZT thin film is then formed by sol–gel deposition [22]. The PZT thin film has a (100)/(001) preferred orientation which gives a larger piezoelectric constant compared with (111) oriented ones [23]. The cross-sectional scanning electron microscope (SEM) image of the PZT thin film deposited by the sol–gel process and the X-ray diffraction (XRD) pattern are shown in Figs. 3a and b, respectively. Then Pt (0.2 µm)/Ti (0.05 µm) thin films are deposited as the top electrode layer by DC magnetron sputtering. Later on, three top electrodes are patterned and etched using Ar ions through mask 1. The PZT thin films are wet-etched using a mixture of HF, HNO$_3$ and HCl through mask 2. Through mask 3, bottom electrodes are formed using Ar ions again. Then, through mask 4 the thermal oxide layer and the structural Si layer are etched by reactive ion etching using CHF$_3$ gas (for SiO$_2$) and SF$_6$ (for Si). Finally, the handle Si layer and BOX layer are etched from the backside to release the PZT microcantilever. A photograph of the fabricated PZT microcantilever with a whole chip size of 5.0 mm × 4.2 mm × 0.4 mm is shown in Fig. 1b. The fabricated chip is later on assembled and wire-bonded to a metal package for the sake of dynamic characterisation.

3. Flow-sensing capability: An air-flow testing system as shown in Fig. 4 is utilised to characterise the flow-sensing capability. In the system, a compressed air source is connected to a flow channel with a diameter of 3.5 mm. The air flow rate in the channel can be changed by a flow meter to imitate ambient wind flow of different levels. As the flow rate Q varies from 2 to 9 slm
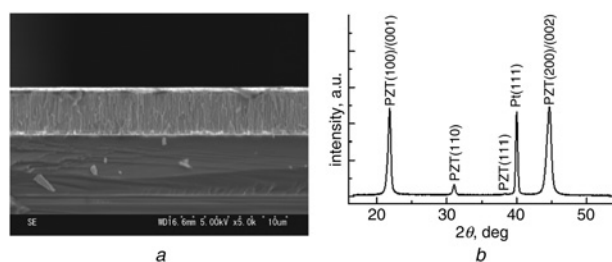
(litre/min), the flow velocity v_f can be derived according to $v_f = Q/A$, where A is the flow area related to the diameter of the flow channel. To prevent wind scattering, the packaged PZT

Figure 5 *Output rms voltages of the PZT microcantilever against flow velocities varying from 3.5 to 15.6 m/s (Fig. 5a) and instantaneous output waveform at flow velocity of 5.2 m/s and (Figs. 5b and c, respectively)*

Figure 3 *Cross-sectional SEM image of the PZT thin film deposited by sol–gel process and the XRD pattern of the deposited PZT thin film*
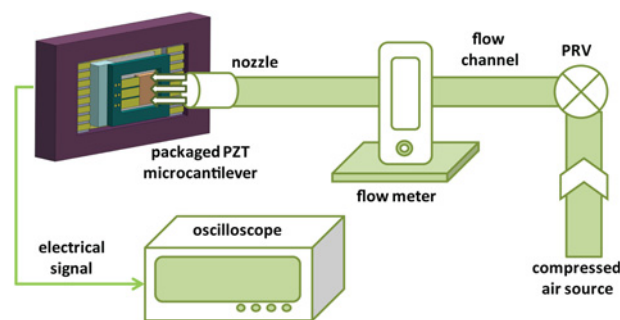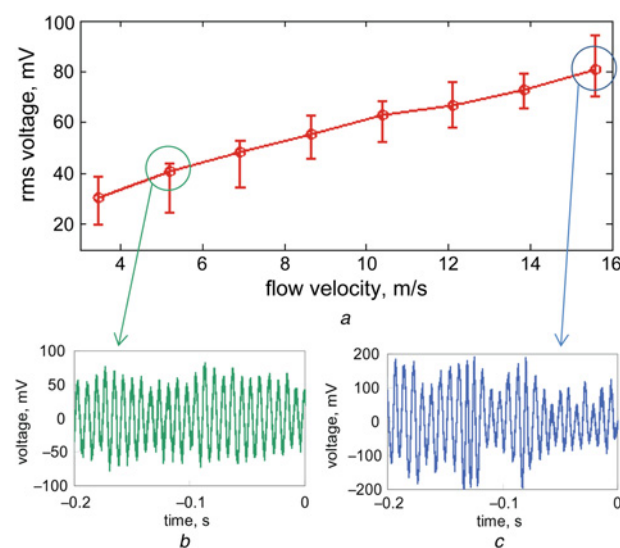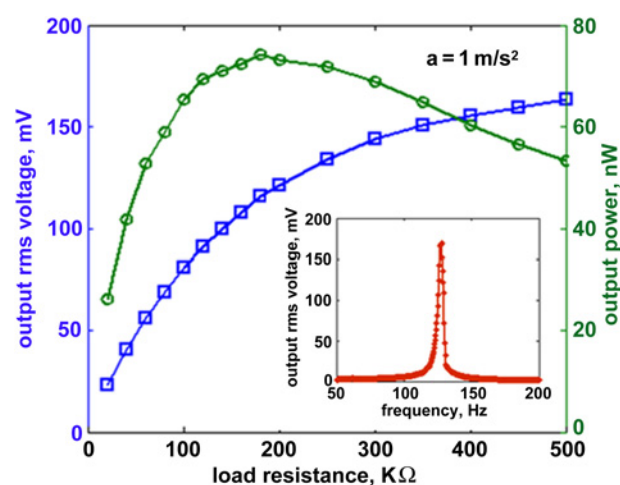*a Cross-sectional SEM image*
b XRD pattern

Figure 6 *Output rms voltage and power against load resistance for excitation frequency of 127 Hz and input acceleration of 1 m/s^2*
Inset figure shows the output rms voltage against excitation frequency at input acceleration of 1 m/s^2

Table 1 Summary of the maximum load rms voltages, optimised power and power densities at different flow velocities regarding a matched load resistance of 180 kΩ

Flow velocity, m/s		3.5	5.2	6.9	8.7	10.4	12.1	13.8	15.6
PZT thin film component 1	load rms voltage, mV	19.2	24.7	30.5	35.5	38.4	41.2	45.6	48.1
	output power, nW	2.1	3.4	5.2	7.0	8.2	9.4	11.6	12.9
Three PZT thin films component	output power, nW	6.3	10.2	15.6	21.0	24.6	28.2	34.8	38.7
	power density, μW/cm^3	4.5	7.5	11.4	15.6	18.3	21.0	25.5	28.5

microcantilever is placed at 10 mm away from the nozzle of the flow channel. Due to the small chip size, the PZT microcantilever is almost entirely immersed within the air-flow boundary. The air flow at the microcantilever is in the transition stage between the pipe flow and the open channel flow. To verify the flow velocity during that transition, the finite element modelling (FEM) was conducted by ANSYS Fluent. From the modelling results, the flow velocity drops to approximately 95% of that of the channel (range of 0–25 m/s). As a result, all values of flow velocity plotted in Fig. 5 and Table 1 are the results after considering an average velocity degrading of 5% during the flow transition.

In this case, a turbulence-induced vibration will occur with a modulated vibration response nearby its resonant frequency [24, 25]. Subsequently, the three PZT thin film components experience the same strain variations and generate the same amount of electricity. In this measurement, only PZT thin film component 1 is connected to a digital signal oscilloscope. Fig. 5a shows the mean, maximum and minimum rms voltages of the flow sensor (indicated by error bars) against flow velocity varying from 3.5 to 15.6 m/s. As can be seen, the output voltage of the flow sensor increases steadily as the flow velocity increases. This is because the viscous flow induced dragging force acting on the PZT microcantilever increases with air flow velocity according to fluid dynamics [26]. By calculating the slope of the mean rms voltages, the average sensitivity of the flow sensor is observed as 4.2 mV per unit change of flow velocity. Figs. 5b and c show the instantaneous voltage waveforms of the flow sensor at flow velocities of 5.2 and 15.6 m/s, respectively, while because of the turbulence-induced vibration, there are irregular oscillation amplitudes and thus voltage spectra at different flow velocities, but all have similar modulated oscillation responses nearby its resonant frequency of 127 Hz.

4. Energy harvesting capability: A vibration testing system is utilised to measure the vibration-driven energy harvesting capability. The testing setups consist of a vibration shaker, an amplifier and a dynamic signal analyser. As shown in the most of Fig. 6, a peak rms voltage of 170 mV is obtained at the resonant frequency of 127 Hz for an input acceleration of 1 m/s^2. Fig. 5 shows the output rms voltages and power against load resistance at the resonant frequency of 127 Hz and an acceleration of 1 m/s^2. It is observed that when the load resistance reaches 180 kΩ, the output power achieves a maximum value of 74.2 nW. It means for an operating frequency of 127 Hz, the load resistance of 180 kΩ is matched with the internal impedance of the piezoelectric microcantilever. As can be seen from Figs. 5b and c, the turbulence-induced vibration of the microcantilever is nearby its resonant frequency of 127 Hz at different flow velocities. Hence, an optimised load resistor of 180 kΩ is deployed in the flow testing for characterisation of the wind-driven energy harvesting capability. For PZT thin film component 1, the load rms voltages, and the maximum power delivered to the matched load resistance of 180 kΩ are summarised in Table 1 with respect to flow velocity varying from 3.2 to 14.5 m/s.

The maximum total output power for three PZT thin film components is obtained as well, where it is about three times higher

than that of one PZT thin film component [27]. The corresponding power densities are derived and shown in Table 1. As can be seen from the Table, the load rms voltage increases gradually with the increment of flow velocity. This is in accordance with the results of flow sensing as shown in Fig. 5. The air flow sensor is tested under a range of air speeds from 3.2 to 14.5 m/s with the flow sensing resolution about 4.5 m/s. Such a sensing range corresponds to wind levels of 3–7 on the Beaufort scale, which cover almost all the indoor and outdoor wind flow available. The power densities of 4.5–28.5 μW/cm^3 have been achieved in the above-mentioned wind flow range. Although such power is actually smaller than the power derived at an excitation acceleration of 1 m/s^2, the proposed wind-driven energy harvesting approach completely eliminates the operation bandwidth issue that vibration-driven energy harvesting mechanism only achieves its maximum output power at its mechanical resonant frequency.

5. Concluding remarks: A wind-driven piezoelectric PZT microcantilever is characterised in terms of flow sensing and energy harvesting capability. Since the piezoelectric sensing mechanism is a passive approach, an efficient autonomous sensing can be realised in a low power consumption manner. Meanwhile, unlike the conventional wind turbine, a piezoelectric MEMS wind-driven energy harvester is much smaller in size and hence is more suitable for low power autonomous sensors. With further research effort in microsystem optimisation, a self-sustained flow-sensing autonomous microsystem for various applications is possible by employing one PZT microcantilever for flow sensing and integrating an array of microcantilevers for providing sufficient power from wind-driven vibrations to maintain the whole microsystem.

7 References

[1] Weimer M.A., Paing T.S., Zane R.A.: 'Remote area wind energy harvesting for low-power autonomous sensors'. 37th IEEE Power Electronics Specialists Conf., 2006, pp. 2911–2915

[2] Tan Y.K., Panda S.K.: 'A novel piezoelectric based wind energy harvester for low-power autonomous wind speed sensor'. 33rd Annual Conf. of the IEEE Industrial Electronics Society (IECON'07), Taiwan, 2007, pp. 2175–2180

[3] Liu H., Zhang S., Kathiresan R., Kobayashi T., Lee C.: 'Development of piezoelectric microcantilever flow sensor with wind-driven energy harvesting capability', *Appl. Phys. Lett.*, 2012, **100**, p. 233905

[4] Li C., Wu P.-M., Hartings J., *ET AL.*: 'Smart catheter flow sensor for real-time continuous regional cerebral blood flow monitoring', *Appl. Phys. Lett.*, 2011, **99**, p. 233705

[5] Kim T.H., Kim S.J.: 'Development of a micro-thermal flow sensor with thin-film thermocouples', *J. Micromech. Microeng.*, 2006, **16**, (11), pp. 2502–2508

[6] Zhang S., Lou L., Lee C.: 'Piezoresistive silicon nanowire based nanoelectromechanical system cantilever air flow sensor', *Appl. Phys. Lett.*, 2012, **100**, p. 023111

[7] Enoksson P., Stemme G., Stemme E.: 'Silicon resonant sensor structure for Coriolis mass-flow measurements', *J. Microelectromech. Syst.*, 1997, **6**, (2), pp. 119–125

[8] Chen N., Tucker C., Engel J.M., Yang Y., Pandya S., Liu C.: 'Design and characterization of artificial haircell sensor for flow sensing with ultrahigh velocity and angular sensitivity', *J. Microelectromech. Syst.*, 1997, **16**, (5), pp. 999–1014

[9] Stemme G.: 'Resonant silicon sensors', *J. Micromech. Microeng.*, 1991, **1**, (2), pp. 113–125

[10] Priya S., Chen C.-T., Fye D., Zahnd J.: 'Piezoelectric windmill: a novel solution to remote sensing', *Jpn. J. Appl. Phys.*, 2005, **44**, (3), pp. L104–L107

[11] Priya S.: 'Modeling of electric energy harvesting using piezoelectric windmill', *Appl. Phys. Lett.*, 2005, **87**, (18), p. 184101

[12] Myers R., Vickers M., Kim H.: 'Small scale windmill', *Appl. Phys. Lett.*, 2007, **90**, (5), p. 054106

[13] Kwon S.-D.: 'A T-shaped piezoelectric cantilever for fluid energy harvesting', *Appl. Phys. Lett.*, 2010, **97**, (16), p. 164102

[14] Ovejas V.J., Cuadras A.: 'Multimodal piezoelectric wind energy harvesters', *Smart Mater. Struct.*, 2011, **20**, (8), p. 085030

[15] Li S., Yuan J., Lipson H.: 'Ambient wind energy harvesting using cross-flow fluttering', *J. Appl. Phys.*, 2011, **109**, (2), p. 026104

[16] Kim S.-H., Ji C.-H., Galle P., ET AL.: 'An electromagnetic energy scavenger from direct airflow', *J. Micromech. Microeng.*, 2009, **19**, (9), p. 094010

[17] Clair D. St., Bibo A., Sennakesavababu V.R., Daqaq M.F., Li G.: 'A scalable concept for micropower generation using flow-induced self-excited oscillations', *Appl. Phys. Lett.*, 2010, **96**, (14), p. 144103

[18] Matova S.P., Elfrink R., Vullers R.J.M., van Schaijk R.: 'Harvesting energy from airflow with a michromachined piezoelectric harvester inside a Helmholtz resonator', *J. Micromech. Microeng.*, 2011, **21**, (10), p. 104001

[19] Liu H., Tay C.J., Quan C., Kobayashi T., Lee C.: 'A scrape-through piezoelectric MEMS energy harvester with frequency broadband and up-conversion behaviors', *Microsyst. Technol.*, 2011, **17**, (12), pp. 1747–1754

[20] Liu H., Lee C., Kobayashi T., Tay C.J., Quan C.: 'Investigation of a MEMS piezoelectric energy harvester system with a frequency-widened-bandwidth mechanism introduced by mechanical stoppers', *Smart Mater. Struct.*, 2012, **21**, (3), p. 035005

[21] Liu H., Lee C., Kobayashi T., Tay C.J., Quan C.: 'A new S-shaped MEMS PZT cantilever for energy harvesting from low frequency vibrations below 30 Hz', *Microsyst. Technol.*, 2012, **18**, (4), pp. 497–506

[22] Kobayashi T., Ichiki M., Tsaur J., Maeda R.: 'Effect of multi-coating process on the orientation and microstructure of lead zirconate titanate (PZT) thin films derived by chemical solution deposition', *Thin Solid Films*, 2005, **489**, (1–2), pp. 74–78

[23] Taylor D.V., Damjanovic D.: 'Piezoelectric properties of rhombohedral Pb(Zr, Ti)O$_3$ thin films with (100), (111), and "random" crystallographic orientation', *Appl. Phys. Lett.*, 2000, **76**, (12), pp. 1615–1617

[24] Seo Y.H., Kim B.H.: 'A self-resonant micro flow velocity sensor based on a resonant frequency shift by flow-induced vibration', *J. Micromech. Microeng.*, 2010, **20**, (7), p. 075024

[25] Blevins R.D.: 'Flow-Induced Vibration' (Van Nostrand-Reinhold, Princeton, NJ, 1977)

[26] Gerhart P.M., Gross R.J., Hochstein J.I.: 'Fundamentals of fluid mechanics' (Addison-Wesley, Reading, MA, 1992)

[27] Liu H., Tay C.J., Quan C., Kobayashi T., Lee C.: 'Piezoelectric MEMS energy harvester for low-frequency vibrations with wideband operation range and steadily increased output power', *J. Microelectromech. Syst.*, 2011, **20**, (5), pp. 1131–1142